Tests of General Relativity with Gravitational Waves

Valentino Huang
huangv@student.ethz.ch

June 2021

Supervisor: Prof. Philippe Jetzer
Internal member of ETH: Prof. Gian Michele Graf

Abstract General relativity and some alternative theories of gravity predict gravitational waves. With their first detection in 2015 those theories can now be tested. In this work we first give a theoretical overview of gravitational waves. Then we present some of the most recent results in testing general relativity and possible deviations with data from LIGO and Virgo. To date no significant deviations have been found. Tests on the polarization content find Bayes' factors of more than 200 and 1000 in favour of models with pure tensor polarization over models with pure vector and scalar polarization, respectively. Although first long-time observations give $\ln \mathcal{O}_{\mathrm{N}}^{\mathrm{SIG}} = -0.53$, which indicates a nondetection of the stochastic gravitational-wave background, the total background power of each polarization content has been restricted. Also deviations on the propagation of gravitational waves have been limited successfully. The speed of gravitational waves has been bounded to $-3\times10^{-15} \leq \Delta v/c \leq +7\times10^{-16}$ and the upper limit for the graviton mass has been calculated to be $m_g \leq 1.76\times10^{-23}\,\mathrm{eV}/c^2$. Hence also Lorentz-invariance has been strengthened. Waveform tests don't show any deviations from theory. Residuals after subtracting the best-fit waveform mostly seem to come from instrumental Gaussian noise. The differences of the inferred mass and spin from the inspiral and postinspiral phase of GWTC-2 BBH mergers, $\Delta M_{\mathrm{f}}/\bar{M}_{\mathrm{f}} = 0.02^{+0.20}_{-0.17}$ and $\Delta\chi_{\mathrm{f}}/\bar{\chi}_{\mathrm{f}} = -0.05^{+0.36}_{-0.41}$, are quite consistent with the zero values from general relativity. The no-hair conjecture seems to hold to the best of our knowledge.

Contents

1 Introduction

More than a century after its prediction general relativity is still the best theory we have to describe gravity and has therefore become one of the great pillars of modern physics. Nevertheless, Einstein's theory has some serious issues in very small and very large scales. The persistent difficulty of quantization and the mysteries of cosmic inflation and dark energy lead physicists to develop numerous alternative theories of gravitation. Unfortunately, to date none of them could be confirmed experimentally. On the other hand, over the years more and more observations have shown stunning agreement with the predictions of general relativity. In 2015 with the first detection of gravitational waves the next step has been made. Einstein already predicted the existence of gravitational waves in 1916. These waves, generated by time-varying quadrupole moments of a mass distribution propagate at the speed of light and locally deform spacetime. Their detection opens a whole new world of possibilities to test general relativity and its limits.

So far we could only test gravity indirectly, by deducting the motion and properties of sources in the sky through measurements of electromagnetic waves and with the help of our astrophysical knowledge. Now we can "see" the effect of gravity directly be measuring these perturbations in spacetime. The mere existence of gravitational waves is yet another argument which strengthens general relativity, but over the years other theories which predict their existence have been developed and maybe, if all of these were proven wrong, we still need another theory which hasn't been developed yet. Gravitational waves can be used to test these theories in a few different ways. In this paper we want to go through some of them and summarize what impact five years of experiment have already made on general relativity and its contending theories of gravity.

2 Theory of gravitational waves

2.1 General relativity

2.1.1 Linearized gravity

This section mainly follows the lecture notes of Philippe Jetzer [26] and the work of Alessandra Buonanno [15] and Matthias Blau [14]. Among the most important statements of Einstein's theory of general relativity are the Einstein field equations

$$R_{\mu\nu} = -\frac{8\pi G}{c^4}\Big(T_{\mu\nu} - \frac{T}{2}g_{\mu\nu}\Big). \tag{1}$$

Assuming both a weak gravitational field and a static gravitational field the Newtonian limit can be recovered. However, if we only impose that the field is weak,

$$g_{\mu\nu} = \eta_{\mu\nu} + h_{\mu\nu}, \qquad |h_{\mu\nu}| \ll 1, \tag{2}$$

other interesting physics is revealed. This limit is called linearized gravity. Dropping the higher order terms the Ricci tensor of first order in h becomes

$$R^{(1)}_{\mu\nu} = \frac{1}{2}(\Box h_{\mu\nu} + h_{,\mu,\nu} - h^{\sigma}_{\mu,\nu,\sigma} - h^{\sigma}_{\nu,\mu,\sigma}).$$

Thus the linearized version of (1) can be written as

$$\Box h_{\mu\nu} + h_{,\mu,\nu} - h^{\sigma}_{\mu,\nu,\sigma} - h^{\sigma}_{\nu,\mu,\sigma} = -\frac{16\pi G}{c^4}\Big(T^{(1)}_{\mu\nu} - \frac{T^{(1)}}{2}\eta_{\mu\nu}\Big). \tag{3}$$

2.1.2 Gauge invariance

General relativity is a theory which is invariant under the group of all possible coordinate transformations

$$x^{\mu} \to x'^{\mu}(x^{\mu}),$$

where the transformation is a diffeomorphism (differentiable and invertible with differentiable inverse). Under such a generic transformation the metric tensor field transforms as

$$g_{\mu\nu}(x) \to g'_{\mu\nu}(x') = \frac{\partial x^{\rho}}{\partial x'^{\mu}}\frac{\partial x^{\sigma}}{\partial x'^{\nu}}g_{\rho\sigma}.$$

This follows from the statement that the line element should be the same in any coordinate frame

$$\mathrm{d}s^2 = g_{\rho\sigma}\mathrm{d}x^{\rho}\mathrm{d}x^{\sigma} = g_{\rho\sigma}\frac{\partial x^{\rho}}{\partial x'^{\mu}}\frac{\partial x^{\sigma}}{\partial x'^{\nu}}\mathrm{d}x'^{\mu}\mathrm{d}x'^{\nu}.$$

By choosing the metric to be a small perturbation of flat space as in equation (2) we break general covariance since we move into a particular frame. However, there is still a residual gauge symmetry left. This is the gauge symmetry of linearized gravity. Consider the transformation

$$x^{\mu} \to x'^{\mu} = x^{\mu} + \varepsilon^{\mu}, \qquad \varepsilon \ll 1 \tag{4}$$

Then we get

$$\frac{\partial x^{\rho}}{\partial x'^{\mu}} = \delta^{\rho}_{\mu} - \partial_{\mu}\varepsilon^{\rho}.$$

The transformed field is up to first order

$$\begin{aligned} g'_{\mu\nu} &= (\delta^\rho_\mu - \partial_\mu \varepsilon^\rho)(\delta^\sigma_\nu - \partial_\nu \varepsilon^\sigma) g_{\rho\sigma} \\ &= (\delta^\rho_\mu \delta^\sigma_\nu - \delta^\rho_\mu \partial_\nu \varepsilon^\sigma - \delta^\sigma_\nu \partial_\nu \varepsilon^\rho + \partial_\mu \varepsilon^\rho \partial_\nu \varepsilon^\sigma)(\eta_{\rho\sigma} + h_{\rho\sigma}) \\ &= \eta_{\mu\nu} + h_{\mu\nu} - \eta_{\mu\sigma}\partial_\nu \varepsilon^\sigma - \eta_{\rho\nu}\partial_\mu \varepsilon^\rho - h_{\mu\sigma}\partial_\nu \varepsilon^\sigma - h_{\rho\nu}\partial_\mu \varepsilon^\rho + \eta_{\rho\sigma}\partial_\mu \varepsilon^\rho \partial_\nu \varepsilon^\sigma + h_{\rho\sigma}\partial_\mu \varepsilon^\rho \partial_\nu \varepsilon^\sigma \\ &\approx \eta_{\mu\nu} + h_{\mu\nu} - \partial_\nu \varepsilon_\mu - \partial_\mu \varepsilon_\nu. \end{aligned}$$

Assuming that this transformation preserves the form of (2) we get $g'_{\mu\nu} = \eta_{\mu\nu} + h'_{\mu\nu}$. And so the field transforms as

$$h'_{\mu\nu} = h_{\mu\nu} - \frac{\partial \varepsilon_\mu}{\partial x^\nu} - \frac{\partial \varepsilon_\nu}{\partial x^\mu}. \tag{5}$$

Here we simplified a little bit in the sense that we assumed that (4) was a symmetry of (2). This assumption is intuitively justified, because only small shifts in spacetime can leave the form of the metric close to flat space. However, the correct way to see this is by looking at all possible transformations which leave h sufficiently small. This is fully shown in the appendix A.

2.1.3 Gauge fixing

A possible gauge fixing is the harmonic gauge (also Lorenz or De Donder gauge) which is given by the condition

$$2h^\mu_{\nu,\mu} = h^\mu_{\mu,\nu}. \tag{6}$$

Note that if h does not satisfy this condition then there exists a suitable gauge transformation of the form (5) which gives a field that satisfies the condition. These gauge transformations are given by all vector fields ε^μ that satisfy

$$\Box \varepsilon_\nu = -h^\mu_{\nu,\mu} + \frac{1}{2} h^\mu_{\mu,\nu}. \tag{7}$$

Differentiation of (6) with respect to x^μ leads to

$$h_{,\mu,\nu} - h^\sigma_{\mu,\nu,\sigma} - h^\sigma_{\nu,\mu,\sigma} = 0.$$

Inserting this into (3) gives the decoupled linearized field equations

$$\Box h_{\mu\nu} = -\frac{16\pi G}{c^4}\Big(T_{\mu\nu} - \frac{T}{2}\eta_{\mu\nu}\Big).$$

In the vacuum one has $T_{\mu\nu} = 0$ and thus the source-term vanishes leaving the wave equation

$$\Box h_{\mu\nu} = 0.$$

Solutions of this equation are plane waves of the type

$$h_{\mu\nu} = e_{\mu\nu}(\vec{k}) \exp\left(-i k_\rho x^\rho\right) \tag{8}$$

with $k_\mu k^\mu = 0$. Since $h_{\mu\nu}$ is symmetric also the polarization tensor $e_{\mu\nu}$ must be symmetric which reduces the number of independent components from 16 to 10. Furthermore one can always choose a coordinate system in which the wave is travelling in positive z-direction, $k^\mu = (k, 0, 0, k)$. Inserting this solution (8) into the gauge condition (6) gives 4 more constraining equations leaving 6 independent components

$$e_{00}, \quad e_{11}, \quad e_{33}, \quad e_{12}, \quad e_{13} \quad \text{and} \quad e_{23}, \tag{9}$$

while the other components are given by

$$e_{01} = -e_{31}, \quad e_{02} = -e_{32}, \quad e_{22} = -e_{11}, \quad e_{03} = -\frac{1}{2}(e_{00} + e_{33}).$$

Our gauge (6) has still some redundant degrees of freedom; we can still choose ε_μ such that

$$\Box\varepsilon_\mu = 0$$

and the condition won't change, as can be seen from (7). Solutions of this are again plane waves

$$\varepsilon^\mu = \delta^\mu(\vec{k}) \exp(-ik_\rho x^\rho), \tag{10}$$

where we have chosen the same wave vector k^μ as before. Inserting equations (8) and (10) into the field transformation (5) gives for the six independent components (9) the equations

$$e'_{11} = e_{11},\ e'_{12} = e_{12},\ e'_{13} = e_{13} - ik\delta_1,\ e'_{23} = e_{23} - ik\delta_2,\ e'_{33} = e_{33} - 2ik\delta_3,\ e'_{00} = e_{00} + 2ik\delta_0.$$

Since for every field δ^μ all these transformed components represent the same physical solution we can simplify the polarization tensor by choosing δ^μ such that $e'_{00} = e'_{13} = e'_{23} = e'_{33} = 0$. This fixes the second gauge condition and is called the transverse-traceless gauge. We end up with

$$h_{\mu\nu} = \begin{pmatrix} 0 & 0 & 0 & 0 \\ 0 & e_{11} & e_{12} & 0 \\ 0 & e_{12} & -e_{11} & 0 \\ 0 & 0 & 0 & 0 \end{pmatrix} \cdot \exp(-ik_\rho x^\rho). \tag{11}$$

This is the most simple description of a gravitational wave travelling in z-direction.

2.2 Alternative theories

Many alternative theories to general relativity have been developed in order to describe physical effects which general relativity fails to describe. Modern theories mainly focus on cosmological aspects, like dealing with inflation, dark matter and dark energy or on unifying gravity with the rest of physics. The most natural way to describe a theory is through its action. If we assume that the Einstein equivalence principle holds, which has strong empirical evidence [34] [35], then the theory we are looking for must be metric. General relativity and its equations follow directly from the Einstein-Hilbert action

$$S = \int R\sqrt{-g}\,\mathrm{d}^4x + S_m(\psi_m, g_{\mu\nu}).$$

One can now add different kind of terms to this action and thus find different kind of theories. Many of these metric theories have already been ruled out [35]. Some theories which are still viable are shortly presented in the following.

2.2.1 Scalar-tensor theories

In scalar-tensor theories [34] the action contains also a scalar field $\varphi(x)$, a potential $V(\varphi)$ and a coupling function $A(\varphi)$

$$S = \int [R - 2g^{\mu\nu}\partial_\mu\varphi\partial_\nu\varphi - V(\varphi)]\sqrt{-g}\,\mathrm{d}^4x + S_m(\psi_m, A^2(\varphi)g_{\mu\nu}).$$

These theories have become very popular in unification schemes. For instance, string theory predicts that the spin-2 graviton has a spin-0 partner called the dilaton, forcing a more precise theory of gravity to be a scalar-tensor theory. Brans-Dicke theory and $f(R)$ theories are popular examples which use both a tensor and a scalar field to mediate gravitational interaction.

2.2.2 Vector-tensor theories

In vector-tensor theories [34] the action contains a four vector field u^μ. This vector might be unconstrained or constrained to be a time-like unit vector (Einstein aether theory). The most general action looks like

$$S = \int [(1 + \omega u_\mu u^\mu)R - K^{\mu\nu}_{\alpha\beta} \nabla_\mu u^\alpha \nabla_\nu u^\beta + \lambda(u_\mu u^\nu + 1)] \sqrt{-g} \mathrm{d}^4x + S_m(\psi_m, g_{\mu\nu}),$$

where

$$K^{\mu\nu}_{\alpha\beta} = c_1 g^{\mu\nu} g_{\alpha\beta} + c_2 \delta^\mu_\alpha \delta^\nu_\beta + c_3 \delta^\mu_\beta \beta^\nu_\alpha - c_4 u^\mu u^\nu g_{\alpha\beta},$$

with arbitrary coefficients c_i.

2.3 Field theoretical point of view

Modern physics tries to incorporate gravity as a fourth force in the Standard Model. This description is called Quantum Gravity (QG). As in the case of the other known forces (electroweak theory and quantum chromodynamics) we would like to describe gravity as a gauge theory. These are theories where the Lagrangian is invariant under transformations of a Lie group, called symmetry group. The interaction between particles is then given by the exchange of gauge bosons, which are excitations of the gauge field. It is an interesting idea, that general covariance can be considered as the gauge symmetry of gravity. The associated gauge boson, called graviton, would then be an excitation of the flat metric field $\eta_{\mu\nu}$. The main problem of QG is that from second order corrections the theory is non-renormalizable.

If the postulated graviton exists, we can already predict some of its properties. Gravity is a long range force which implies that its force carrier should be massless and constantly moving at the speed of light. Furthermore we expect the graviton to be a spin-2 particle since gravity is described by a 2-tensor field. Weinberg already proved in 1965 that every quantum field theory of a massless spin-2 particle would give rise to Einstein's field equation [33]. We could think of gravitational waves to be linear excitation of the graviton field. In that case equation (11) already suggests some of the graviton properties. Since k^μ is a light-like vector ($k^\mu k_\mu = 0$) the graviton moves at the speed of light implying $m_g = 0$. Furthermore we can look at the transformation properties of the polarization tensor. As the name suggests

$$h_{\mu\nu} = \begin{pmatrix} 0 & 0 & 0 & 0 \\ 0 & h_+ & h_\times & 0 \\ 0 & h_\times & h_+ & 0 \\ 0 & 0 & 0 & 0 \end{pmatrix}$$

is a tensor. So under a rotation of angle ϕ around the direction of propagation

$$\Lambda^\mu_\nu = \begin{pmatrix} 1 & 0 & 0 & 0 \\ 0 & \cos\phi & \sin\phi & 0 \\ 0 & -\sin\phi & \cos\phi & 0 \\ 0 & 0 & 0 & 1 \end{pmatrix}$$

it transforms as

$$h'_{\mu\nu} = \Lambda^\rho_\mu \Lambda^\sigma_\nu h_{\rho\sigma}.$$

With

$$\Lambda^2 = \begin{pmatrix} 1 & 0 & 0 & 0 \\ 0 & \cos 2\phi & \sin 2\phi & 0 \\ 0 & -\sin 2\phi & \cos 2\phi & 0 \\ 0 & 0 & 0 & 1 \end{pmatrix}$$

we can see that the transformation rules are

$$h'_\times = \cos(2\phi)h_\times + \sin(2\phi)h_+,$$
$$h'_+ = -\sin(2\phi)h_\times + \cos(2\phi)h_+.$$

Changing into the basis

$$h_{\downarrow,\uparrow} = h_\times \pm ih_+,$$
$$h_\times = \frac{1}{2}(h_\uparrow + h_\downarrow), \qquad h_+ = \frac{i}{2}(h_\downarrow - h_\uparrow)$$

we find that

$$h'_{\downarrow,\uparrow} = e^{\mp 2i\phi}h_{\downarrow,\uparrow}. \tag{12}$$

In particle physics we call helicity the projection of the spin operator onto the direction of propagation $H = \mathbf{S} \cdot \mathbf{n}$. Under a rotation of ϕ around the axis of propagation the helicity eigenstates transform as

$$h \to e^{iH\phi}h.$$

From equation (12) we can see that $h_{\downarrow,\uparrow}$ are helicity eigenstates with $S = 2$. Thus the graviton is a massless spin-2 particle. Being a massless particle it has only two physical projections onto the direction of propagation, which indeed reflects in gravitational waves having only two polarization modes.

3 Detection

3.1 Observatories

In September 2015 the Laser Interferometer Gravitational-Wave Observatory (LIGO) was the first one to detect gravitational waves. LIGO consists of two 4 km long ground-based detectors, one located in Hanford (US) and the other one in Livingston (US). Together with the Virgo interferometer, which is 3 km long and located near Pisa in Italy, they have observed 50 events ever since [1], [9].

At the very core these detectors are Michelson interferometers. They follow the same principle as those in the famous Michelson-Morley experiment in 1887 which would have detected earth's motion through the hypothetical aether. A basic Michelson interferometer consists of a source emitting coherent light (laser), a beam splitter which divides the laser into two orthogonal arms of the same length (which might be variable), mirrors which reflect the laser and send it back through the arms until both beams recombine and a detector which measures the amplitude of the incident light. The difference in optical path length of the two beams will then give either destructive or constructive interference. Thus one can make deductions about the wavelength of the source or materials placed in between one of the arms.

In the case of gravitational waves we want to measure the deformation of space itself. If a gravitational wave passes by it changes the length of the arms according to its direction of propagation. This of course changes the optical path length of the laser in the arms and gives rise to measurable fringes. The more stretched space the laser has to travel through the bigger is the phase difference of the two beams. Thus increasing the length of the arms means increasing the sensibility of detecting very small oscillations in space. The amplitude of a gravitational wave can be defined through the relative difference in length of an object

$$h := 2\frac{l(t) - l_0}{l_0}. \tag{13}$$

To estimate the order of magnitude of this amplitude predicted by general relativity we can use the post-Newtonian approximation. A simple way is presented in [32]. To calculate the change of the

gravitational field as a function of distance of a massive system one can use multipole expansion. Similar to electromagnetism the zeroth order (spherical) monopole term is zero due to conservation of mass and energy. But unlike in electromagnetism also the dipole term vanishes, since it would derive from an oscillation of the center of mass, which would violate momentum conservation. So the leading angular term is the quadrupole moment. Simple estimates for a neutron star in the Virgo cluster give

$$h \sim 10^{-21}.$$

This means that our detector must be able to measure changes in distance of one part in 10^{21}. In order to achieve this, LIGO uses Fabry-Peròt cavities. These are parallel mirrors placed at both ends of the arms which reflect the laser beams back and fort approximately 280 times. This increases the sensibility of the interferometer to small perturbations.

3.2 Detecting gravitational waves

Gravitational waves are created in strongly curved regions of spacetime where heavy masses are accelerated. These waves then move at the speed of light until they reach us as small perturbations. On earth our spacetime can assumed to be flat, $T_{\mu\nu} = 0$, so that these perturbations are of the form (11). When such a wave passes by it deforms spacetime according to

$$\mathrm{d}s^2 = g_{\mu\nu}\mathrm{d}x^\mu \mathrm{d}x^\nu = (\eta_{\mu\nu} + h_{\mu\nu})\mathrm{d}x^\mu \mathrm{d}x^\nu.$$

This deformation will produce an electric signal $h_{\mathrm{out}}(t)$ in the detector, the so-called response function. This is nothing else than the strain from equation (13) as a function of time. The most promising sources of detection are the so-called gravitational-wave transients. These are single peaked signals generated by high-energy events like compact binary coalescences (CBCs), including binary black hole (BBH) mergers, binary neutron star (BNS) mergers and neutron star-black hole (NS-BH) mergers. An example of a visual data set of a BBH merger is shown in Figure 1. This was the first ever measurement of LIGO Hanford and LIGO Livingston, known as GW150814 (since detected on August 14th 2015). The top row shows the output strain $h_{\mathrm{out}}(t)$ measured by the two detectors. More details can be found in [4].

4 Tests of polarization

A prediction of general relativity is the existence of only two polarizations, the cross and plus modes

$$e_+ = \begin{pmatrix} 1 & 0 & 0 \\ 0 & -1 & 0 \\ 0 & 0 & 0 \end{pmatrix}, \qquad e_\times = \begin{pmatrix} 0 & 1 & 0 \\ 1 & 0 & 0 \\ 0 & 0 & 0 \end{pmatrix}.$$

Assuming only metric theories the number of possible polarizations is constrained to be at most six. So in general other gravitational theories allow up to four additional polarizations, the x and y vector modes and the breathing and longitudinal scalar modes [6], [28]

$$e_x = \begin{pmatrix} 0 & 0 & 1 \\ 0 & 0 & 0 \\ 1 & 0 & 0 \end{pmatrix}, \qquad e_y = \begin{pmatrix} 0 & 0 & 0 \\ 0 & 0 & 1 \\ 0 & 1 & 0 \end{pmatrix}, \qquad e_b = \begin{pmatrix} 1 & 0 & 0 \\ 0 & 1 & 0 \\ 0 & 0 & 0 \end{pmatrix}, \qquad e_l = \begin{pmatrix} 0 & 0 & 0 \\ 0 & 0 & 0 \\ 0 & 0 & 1 \end{pmatrix}.$$

This means that finding one of the last four polarizations would violate general relativity and favour an alternative gravitational theory. The deformation of a ring of free falling particles under the effect of these polarization modes is shown in Figure 2. In principle every combination of the above polarizations is allowed in general gravitational theories. At every point in spacetime x the metric perturbation can be written as

$$h_{ij}(x) = h_a(x) e^a_{ij} = \begin{pmatrix} h_+ + h_b & h_\times & h_x \\ h_\times & -h_+ + h_b & h_y \\ h_x & h_y & h_l \end{pmatrix},$$

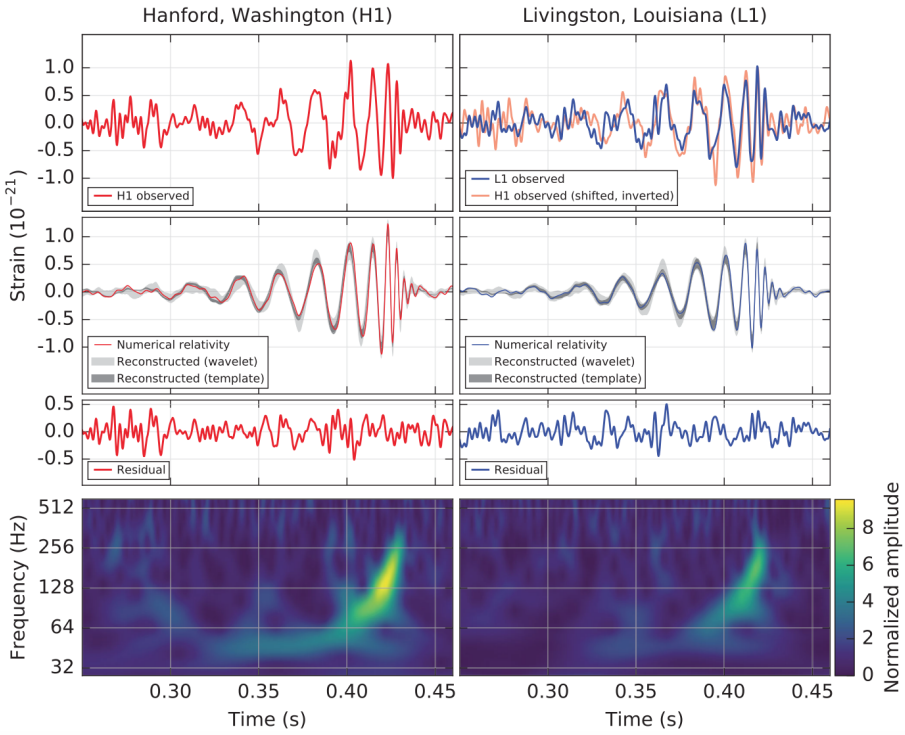

Figure 1: The gravitational-wave event GW150814 observed by LIGO Hanford (H1, left column) and LIGO Livingston (L1, right column). *Top row:* the gravitational wave strain measured by the two interferometers. *Second row:* the simulated strain with inferred parameters of this BBH merger using numerical relativity. The shaded regions show the 90%-credibility regions for two different models. *Third row:* Residual noise after subtracting the numerical waveform from the detector measurements. *Bottom row:* a time-frequency representation of the data, showing which frequency bands are dominant.

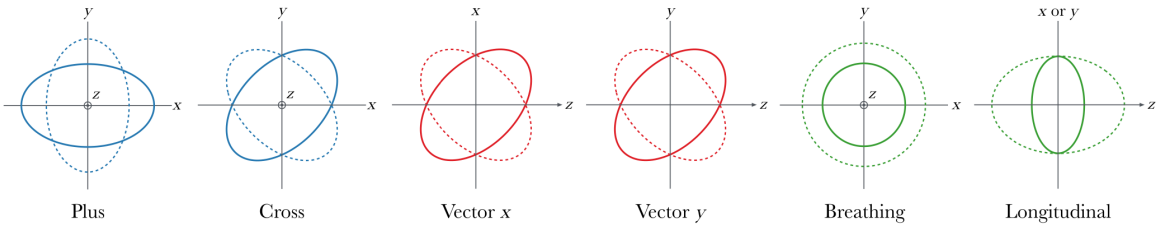

Figure 2: The effect of all six gravitational wave polarization modes on a ring of free falling particles. The wave is always propagating in z-direction.

where we summed over all the polarizations a and only considered the spatial part $i, j \in \{1, 2, 3\}$. There are several factors which limit the study of the polarization of gravitational wave transients. First of all, the detectors of LIGO-Hanford and LIGO-Livingston are nearly co-oriented, preventing Advanced LIGO from measuring more than a single polarization mode. Secondly, even if the detectors were more favourably oriented a network of at least six detectors is needed to fully characterize the polarization content of a gravitational wave transient [16]. It should be noted that using quadrupolar detectors like LIGO and Virgo the two scalar modes, longitudinal and breathing, give completely degenerate responses. So a network of quadrupolar detectors can measure at most five different independent polarization degrees of freedom. We can simplify things by splitting all combinations into models of pure polarization states, i.e. pure tensor, pure vector and pure scalar modes and into models of mixed polarization states.

4.1 Pure modes

These models limit the number of polarization modes to be at most two. This makes it possible to analyse them by observing gravitational-wave transients with both LIGO and Virgo. The data of the event GW170814 [5], which was a BBH merger and the first signal detected by LIGO and Virgo together, strongly favours pure tensor polarization over pure vector or pure scalar polarizations. The methodology used to compare theory with experiment is based on how the polarization of a gravitational wave affects the response function of ground-based detectors [18]. Different polarizations have different impacts on the relative strain. This can be quantified in form of the antenna pattern F, which is a purely geometric quantity. In the following we use the coordinate frame where one interferometer arm lies on the x-axis and the other one on the y-axis. Let (θ, ϕ) be the direction of the source and ψ be the polarization angle. The response function for tensor polarized waves is then

$$h(t) = F^{+} h_{+} + F^{\times} h_{\times},$$

with the tensor antenna patterns

$$F^{+} = \frac{1}{2}(1 + \cos^2\theta)\cos 2\phi \cos 2\psi - \cos\theta \sin 2\phi \sin 2\psi$$

$$F^{\times} = \frac{1}{2}(1 + \cos^2\theta)\cos 2\phi \sin 2\psi - \cos\theta \sin 2\phi \cos 2\psi.$$

In the search for gravitational-wave polarizations done in [5] Bayesian analysis is used once with the standard tensor antenna response functions and then repeated with the appropriate response functions for scalar and vector polarizations. The results show Bayes' factors of more than 200 in favour of pure tensor polarizations over pure vector polarizations and more then 1000 times in favour over pure scalar polarizations. This is a clear evidence which strengthens general relativity over other models with alternative polarizations.

4.2 Mixed modes

In this section we present a viable alternative to the detection of strong binary coalescences with the study of the stochastic gravitational-wave background, presented in full glory in [16] and [25]. The stochastic gravitational-wave background is generated by the superposition of all gravitational-wave sources which are too weak or too distant to individually resolve. In order to detect and study the stochastic gravitational-wave background we have to make minimal assumptions about the background and basically none about the sources itself. The measured quantity is the cross-correlation

$$\hat{C}(f) \propto \tilde{s}_1^{*}(f)\tilde{s}_2(f), \tag{14}$$

between the strains $\tilde{s}_1(f)$ and $\tilde{s}_2(f)$ measured by two different detectors. These are nothing else than the measured amplitude as a function of the frequency f. We assume that the stochastic background

is isotropic (no preferred direction with respect to earth), stationary and Gaussian. Furthermore we assume that there is no correlation between different types of polarization, so that the correlation in (14) can be written as a sum over the polarization type

$$\hat{C}(f) \propto \tilde{s}^*_{1,a}(f)\tilde{s}^a_2(f),$$

with $a \in \{T, V, S\}$. Finally, we assume that tensor and vector modes are individually unpolarized. This follows from our isotropy assumption. Since $\{e_+, e_\times\}$ and also $\{e_x, e_y\}$ can be rotated into each other by a coordinate transformation and we assumed that they are randomly oriented with respect to earth we expect no preferred mode within the same type. This doesn't hold for scalar modes since they can not be transformed into each other. However, as stated above, our detectors are only sensitive to the total scalar power and can not resolve breathing and longitudinal modes individually. Certain theories may violate one or more of the previous assumptions. For example in theories violating Lorentz invariance the background will not be isotropic. However, given these assumptions, the total measured cross power due to the background is given by

$$\langle \tilde{s}^*_{1,a}(f)\tilde{s}^a_2(f')\rangle = \delta(f - f')\gamma_a(f)H^a(f).$$

The function $\gamma_a(f)$ is the overlap reduction function which states the sensitivity of the detector pairs to the detection of the isotropic background of the polarization a. The function $H^a(f)$ is an observable quantity which contains the spectral shape of the stochastic background and is theory independent. However, normally it is expressed through the gravitational-wave energy density of the stochastic background defined as the fraction of the critical energy-density contained in gravitational waves per logarithmic frequency interval

$$\Omega(f) = \frac{1}{\rho_C}\frac{\mathrm{d}\rho_{GW}}{\mathrm{d}\ln f}.$$

The relation between the energy-density and the strain power H^a is theory dependent. However, in any theory obeying Isaacson's formula [1] (as general relativity) this relation is given by [11]

$$\Omega(f) = \frac{20\pi^2}{3H_0^2}f^3H(f),$$

where H_0 is the Hubble constant. Although the last formula doesn't hold in general, for simplicity we will use it as a definition for the energy-density spectrum. Now we can choose a normalization of the cross-correlation such that

$$\langle \hat{C}(f)\rangle = \gamma_a(f)H^a(f).$$

However, measuring the cross-correlation is not enough to identify gravitational waves since there is always some motion due to external noise. Therefore we have to define the signal-to-noise ratio (SNR)

$$\mathrm{SNR}^2 = \frac{(\hat{C}|\gamma_a\Omega^a_M)^2}{(\gamma_b\Omega^b_M|\gamma_c\Omega^c_M)},$$

where $\Omega^a_M(f)$ is a model for the energy-density spectrum of the stochastic background and the inner product $(\cdot|\cdot)$ is defined such that SNR is maximized when the model is equal to the true energy-density spectrum. The method which was used in [16] to study the polarization content is based on Bayesian statistics. First we need to construct an odds ratio $\mathcal{O}^{\mathrm{SIG}}_{\mathrm{N}}$ between signal (SIG) and noise (N) to determine if a stochastic background (of any polarization content) has been detected. Then we need a second odds ratio $\mathcal{O}^{\mathrm{NGR}}_{\mathrm{GR}}$ between the hypotheses of alternative theories (NGR), i.e. any polarization content except tensor-only, and general relativity (GR), i.e. only tensor polarization. These odds ratios are the Bayes factors

$$\mathcal{O}^{\mathcal{A}}_{\mathcal{B}} = \frac{P(\hat{C}|\mathcal{A})\pi(\mathcal{A})}{P(\hat{C}|\mathcal{B})\pi(\mathcal{B})} \tag{15}$$

[1] Effective energy-stress tensor for gravitational waves in the transverse-traceless gauge: $T_{\mu\nu} = \frac{1}{32\pi}\langle\partial_\mu h_{\rho\sigma}\partial_\nu h^{\rho\sigma}\rangle$ [23]

Prior	$\log \Omega_0^T$	$\log \Omega_0^V$	$\log \Omega_0^S$	Ω_0^T	Ω_0^V	Ω_0^S
Log uniform	-7.25	-7.20	-6.96	5.58×10^{-8}	6.35×10^{-8}	1.08×10^{-7}
Uniform	-6.70	-6.59	-6.07	2.02×10^{-7}	2.54×10^{-7}	8.44×10^{-7}

Table 1: Results for the Bayesian analysis for a scalar-, vector- and tensor-polarized gravitationa-wave background. This table shows the upper limits on the amplitudes of each polarization content inside the stochastic gravitational-wave background at a reference frequency of $f_0 = 25$ Hz.

for two hypotheses $\mathcal{A}$ and $\mathcal{B}$. $\pi(\mathcal{A})$ is the prior probability of $\mathcal{A}$ and

$$P(\hat{C}|\mathcal{A}) = \int \mathcal{L}(\hat{C}|, \theta_A, \mathcal{A})\pi(\theta_A|\mathcal{A})\mathrm{d}\theta_A \tag{16}$$

is the Bayesian evidence for $\mathcal{A}$ given the data set $\hat{C}(f)$. The likelihood

$$\mathcal{L}(\hat{C}|, \theta_A, \mathcal{A}) \propto \exp\Big[-\frac{1}{2}(\hat{C} - \gamma_a \Omega^a_{\mathcal{A}}|\mathcal{C} - \gamma_a \Omega^a_{\mathcal{A}}\Big] \tag{17}$$

gives the conditional probability to measure the data set $\hat{C}$ under this hypothesis with fixed parameters θ_A. Conventionally models for stochastic energy-density spectra are power laws

$$\Omega^a_M(f) = \Omega^a_0 \Big(\frac{f}{f_0}\Big)^{\alpha_a}, \tag{18}$$

where we sum over the polarizations in the model M and Ω^a_0 is the backgrounds' amplitude at a reference frequency f_0. For instance the model in which all three polarizations exist would be

$$\Omega_{TVS}(f) = \Omega^T_0 \Big(\frac{f}{f_0}\Big)^{\alpha_T} + \Omega^V_0 \Big(\frac{f}{f_0}\Big)^{\alpha_V} + \Omega^S_0 \Big(\frac{f}{f_0}\Big)^{\alpha_S}. \tag{19}$$

The GR hypothesis would then just be given by the tensor amplitude while the NGR hypothesis would be given by the collection of the remaining polarization models:

$$\mathcal{O}^{\mathrm{NGR}}_{\mathrm{GR}} = \sum_{\mathcal{A}\in\{V,S,VS,\dots\}} \mathcal{O}^{\mathcal{A}}_T. \tag{20}$$

The SIG hypothesis is just the collection of all polarization models and the N hypothesis is given by the model where no signal is present ($\Omega_{\mathrm{N}}(f) = 0$):

$$\mathcal{O}^{\mathrm{SIG}}_{\mathrm{N}} = \sum_{\mathcal{A}\in\{T,V,S,\dots\}} \mathcal{O}^{\mathcal{A}}_{\mathrm{N}}. \tag{21}$$

As more and more data comes in, the Bayesian odds are updated according to equation 16. This method was used in [6] with the data of Advanced LIGOs first observational run O1. The resulting values for the odd ratios are $\ln \mathcal{O}^{\mathrm{SIG}}_{\mathrm{N}} = -0.53$, which indicates a nondetection of the stochastic gravitational-wave background, and $\ln \mathcal{O}^{\mathrm{NGR}}_{\mathrm{GR}} = -0.25$, which is a consistent value in the presence of Gaussian noise. Although this nondetection is not able to differentiate between GR and NGR, it can still be used to place upper bounds to the tensor, vector and scalar contribution to the gravitational-wave background. The results for each polarization amplitude is shown in Table 1, which was taken from [6]. Future long-time measurements with more data might lead to a detection of the stochastic gravitational wave background and give insights about its polarization content.

5 Tests of propagation

5.1 Speed of gravitational waves

General relativity predicts that gravitational waves propagate at the speed of light. On the other hand, some scalar-tensor theories predict a propagation speed different than the speed of light [13]. This is due to the fact that the scalar field couples to the metric perturbations via the Weyl tensor, breaking Lorentz invariance.

A huge step in limiting the speed of gravitational waves has been made in 2017 when the event GW170817 was observed by the Advanced LIGO and Virgo collaboration and the gamma-ray burst GRB170817 was observed by the Fermi Gamma-ray Burst Monitor. The full details of the measurements can be found in [3] and [21]. These two observations have been measured almost simultaneously and their sky locations are overlapping. The probability for two different events to occur with such a temporal and spatial similarity is 5.0×10^{-8} [7]. Thus they have been identified to belong to the same physical event, a BNS merger. The observed time delay between the two observations was $(+1.74 \pm 0.05)$ s. We are interested in the difference between the speed of gravitational waves v_g and the speed of light c. For short travel time differences we can write

$$\frac{\Delta v}{c} = \frac{v_g - c}{c} \approx c\frac{\Delta t}{D},$$

where Δt is the travel time difference and D is the distance to the source. Since smaller distances give a less constraining result we will use the lower bound for the 90% credible interval on luminosity distance, which was calculated to be $D = 26$ Mpc. If we assume that the peak of the gravitational wave signal and the first photons were emitted simultaneously the entire time difference which was measured can be attributed to the travel time $\Delta t = (+1.74 \pm 0.05)$ s. This provides an upper bound for Δv. For a lower bound we assume that the gravitational-wave signal was emitted 10 s before the GRB-signal. This results in the constraint for the speed of gravitational waves of

$$-3 \times 10^{-15} \leq \frac{\Delta v}{c} \leq +7 \times 10^{-16}.$$

Previously there have already been made several other restrictions on the speed of gravitational waves. Moore and Nelson showed in 2001 that the absence of gravitational Cherenkov radiation gives a lower bound of $1 - v_g/c \leq 2 \times 10^{-15}$ [30]. More recently, Hulse-Taylor pulsar observations have restricted the speed of gravitational waves to be greater than $0.995c$ [27].

5.2 Graviton mass

In general relativity the mass of the hypothetical graviton should be zero since it propagates along null geodesics with the dispersion relation

$$E^2 = p^2c^2.$$

In alternative theories of gravity the graviton is sometimes endowed with a mass. In order to compare this fact with experimental data we use a phenomenological approach [10] to modify the dispersion relation (first introduced in [29])

$$E^2 = p^2c^2 + A_\alpha (pc)^\alpha, \tag{22}$$

where A_α and α are phenomenological parameters. We consider values for α ranging from 0 to 4 in steps of 0.5, excluding $\alpha = 2$, which would not give any observable dephasing [8]. When every A_α is equal to zero the GR case is recovered. The case of $\alpha = 0$ and $A_0 > 0$ would be a massive term with a graviton mass of

$$m_g = A_0^{1/2} c^{-2}.$$

	m_g	$\lvert\bar{A}_0\rvert$			$\lvert\bar{A}_{0.5}\rvert$			$\lvert\bar{A}_1\rvert$			$\lvert\bar{A}_{1.5}\rvert$			$\lvert\bar{A}_{2.5}\rvert$			$\lvert\bar{A}_3\rvert$			$\lvert\bar{A}_{3.5}\rvert$			$\lvert\bar{A}_4\rvert$		
	$[10^{-23}$ eV/$c^2]$	< $[10^{-45}]$	>	$\mathcal{Q}_{\rm GR}$ [%]	< $[10^{-38}]$	>	$\mathcal{Q}_{\rm GR}$ [%]	< $[10^{-32}]$	>	$\mathcal{Q}_{\rm GR}$ [%]	< $[10^{-26}]$	>	$\mathcal{Q}_{\rm GR}$ [%]	< $[10^{-14}]$	>	$\mathcal{Q}_{\rm GR}$ [%]	< $[10^{-8}]$	>	$\mathcal{Q}_{\rm GR}$ [%]	< $[10^{-2}]$	>	$\mathcal{Q}_{\rm GR}$ [%]	< $[10^{4}]$	>	$\mathcal{Q}_{\rm GR}$ [%]
GWTC-1	4.70	7.99	3.39	79	1.17	0.70	73	2.51	1.21	70	6.96	3.70	86	5.05	8.01	28	2.94	3.66	25	2.01	3.73	35	1.44	2.34	34
GWTC-2	1.76	1.75	1.37	66	0.46	0.28	66	1.00	0.52	79	3.35	1.47	83	1.74	2.43	31	1.08	2.17	17	0.76	1.57	12	0.64	0.88	25

Table 2: Results for the modified dispersion relation analysis. This table shows the 90% credible upper bounds of the graviton mass and the absolute value of the modified dispersion relation parameters A_α and its GR quantiles $\mathcal{Q}_{GR}$. For each parameter A_α the < and > columns show the value when assuming $A_\alpha < 0$ and $A_\alpha > 0$ respectively. The first row shows the results from GWTC-1 and the second row from GWTC-2.

Every other term A_α with $\alpha \neq 0$ would lead to a Lorentz-violating dispersion relation. Such a dispersive relation would have an impact on the speed of the graviton, making it frequency-dependent. The Compton wavelength of the graviton is

$$\lambda_g = \frac{h}{m_g c},$$

with h being the Planck constant. Thus the graviton speed in theories of massive gravity is

$$\frac{v_g^2}{c^2} = \frac{p^2c^2}{E^2} = 1 - \frac{h^2c^2}{\lambda_g^2 E^2},$$

where the energy E depends on the graviton frequency. More generally using (22) the speed of the graviton would be

$$\frac{v_g}{c} = \frac{pc}{E} = 1 - \frac{A_\alpha}{2E^{2-\alpha}} + \mathcal{O}(A_\alpha^2).$$

This means that low frequency gravitons are slower than high frequency gravitons. This can be measured by the detectors through the overall phase difference of a gravitational wave which accumulates during the propagation from the source. The details can be found in [8]. The results of tests with observations from GWTC-1 and GWTC-2 are shown in the Table 2, which was taken from [10]. We note that the latest observations from GWTC-2 restrict the graviton mass to be $m_g \leq 1.76 \times 10^{-23}\,\mathrm{eV}/c^2$, with 90% credibility. This measurement is 2.7 times more stringent compared to those from GWTC-1 and 1.8 compared to those from the most recent Solar System bound of $3.16 \times 10^{-23}\,\mathrm{eV}/c^2$, also with 90% credibility [12].

5.3 Extra dimensions

This section is based on the analysis presented in [2]. In theories of gravity where the number of spacetime dimensions D is greater than 4 there is a difference between the power loss of gravitational waves and electromagnetic waves. This comes from the fact that energy from gravitational waves might leak into large extra dimensions while photons and matter only propagate in four-dimensional spacetime. In general relativity the strain scaling is given by

$$h_{\rm GR} \propto \frac{1}{d_L^{\rm GW}} = \frac{1}{d_L^{\rm EM}},$$

where the luminosity distances d_L for gravitational and electromagnetic radiation are identical. For a general comparison with the measurements we use a phenomenological approach to modify the scaling relation. This model should asymptotically approach general relativity in the strong-field regime and modifications due to leakage in higher dimensions should appear at large distances from the source. One way to achieve this is through a screening mechanism [2]

$$h \propto \frac{1}{d_L^{\rm GW}} = \frac{1}{d_L^{\rm EM}} \left[1 + \left(\frac{d_L^{\rm EM}}{R_c}\right)^n\right]^{-(D-4)/2n},$$

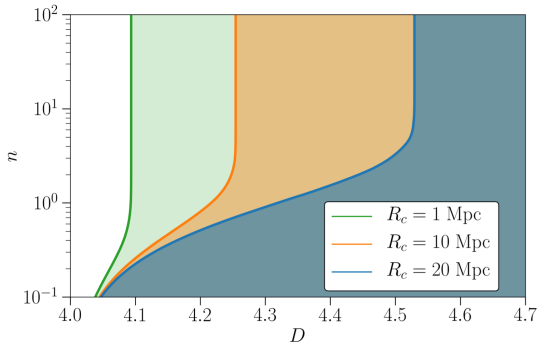

Figure 3: Upper bounds on the number of spacetimes D assuming fixed characteristic length scale R_c and transition steepness n with 90%-credibility. Shaded regions indicate space excluded by the data.

where R_c is the characteristic length scale beyond which gravitational waves start to leak in higher dimensions and n is the transition steepness. We note that for $D = 4$ general relativity is recovered. Results from the Bayesian analysis is shown in Figure 3 [2], which indicate consistency with general relativity prediction $D = 4$.

6 Waveform tests

An important source of information about the strong-field regime is encoded within the waveform of gravitational waves. Some tests concerning the waveform are presented in the following.

6.1 Residual waveform

One method to test general relativity with gravitational waves is to subtract the best-fit waveform from the data and to check if the residuals have the expected statistical properties of the instrumental noise. As an example we can again look at Figure 1. There the first row shows the real strain measurements, while the second row shows the best-fit waveform from the inferred parameters of the BBH. The third row shows the difference between the first 2 rows, called the residual strain.

This section follows the analysis and the results from [8] and [10], in which the null hypothesis, that all detected signals derive from BBH mergers as described by GR, is tested by searching for evidence which might challenge it. An advantage of this method is that it is model-independent, which means that we do not have to compare GR with alternative models but we only check how consistent it is with the data. First Bayesian inference is used to find the best-fit waveform for each detected event. In the mentioned papers for most of these events the Bayesian-inference software libraries LALInference and IMRPhenomPv2 have been used. Now we have to control whether the leftover SNR is consistent with the instrumental noise. The resulting p-values show that the data is consistent with all the residual noise being due to instrumental noise. Figure 4, taken from [10], shows the PP-plot with the p-value on the x-axis and the fraction of events with a p-value less or equal to the corresponding one. For the null-hypothesis, which is that all residual noise is due to instrumental noise, this distribution should be uniform. We can see that the measurements show a similar distribution to the one from the null hypothesis. Thus from this data no evidence for inconsistencies with general relativity are observable.

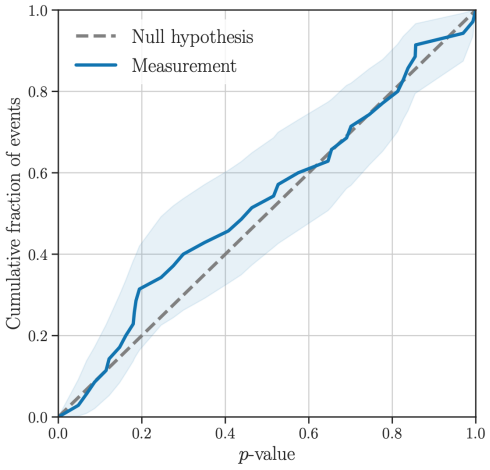

Figure 4: PP-plot for the measured data and the null hypothesis. The null hypothesis is expected to have a uniform distribution of the p-value. For each p-value the blue line marks the fraction of measurements having a residual-test p-value less or equal to it. The light-blue band shows the 90%-credibility regions for the measurements.

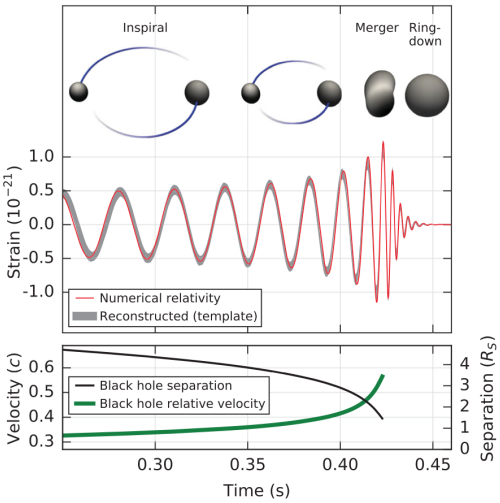

Figure 5: Simulated gravitational-wave form using the inferred source parameters from the first LIGO observation GW150814. With the help of numerical relativity the different phases of a BBH merger are shown by visualizing the event horizon of the two black holes while they coalesce.

6.2 Inspiral-Merger-Ringdown

General relativity predicts that the lifetime of a BBH consists of three stages. During the first stage, called the inspiral, the two black holes will get closer to each other. The orbit of the system will shrink by loosing energy in form of gravitational waves. The beginning of this phase takes a long time and the gravitational-wave emission is very weak. As the orbit shrinks, the black holes will accelerate and the emitted power will increase. The next phase, called the merger, is the time when the two black holes get so close that they meet and combine to a single black hole. When this happens the gravitational-wave emission will have its peak. The third and final phase is the ringdown. After merging together the black hole will oscillate in terms of spherical harmonics until the emission of gravitational waves will smooth it out. The final state of a BBH then consists of a single Kerr black hole, that is a black hole with non-zero angular momentum. Figure 5 shows these stages with the data of the first LIGO observation GW150914 [4].

According to general relativity the mass and spin of the inspiral and post-inspiral stages should be consistent. These phases roughly correspond to the low-frequency and high-frequency spectrum. In [8] and [10] this consistency has been tested. The full methodology is presented in [19]. First the overall mass M_f and dimensionless spin χ_f from the full BBH signal is calculated with the help numerical relativity. The cutoff frequency f_c^IMR, to differentiate between low- and high-frequency regimes, is chosen to be the frequency of the innermost stable circular orbit of a Kerr black hole with the mass M_f and spin χ_f. Then the mass and spin from the inspiral and post-inspiral phases are inferred and confronted with the help of the dimensionless parameters

$$\frac{\Delta M_\mathrm{f}}{\bar{M}_\mathrm{f}} = 2\frac{M_\mathrm{f}^\mathrm{insp} - M_\mathrm{f}^\mathrm{postinsp}}{M_\mathrm{f}^\mathrm{insp} + M_\mathrm{f}^\mathrm{postinsp}}$$

and

$$\frac{\Delta\chi_{\rm f}}{\bar{\chi_{\rm f}}} = 2\frac{\chi_{\rm f}^{\rm insp} - \chi_{\rm f}^{\rm postinsp}}{\chi_{\rm f}^{\rm insp} + \chi_{\rm f}^{\rm postinsp}}.$$

When considered as independent parameters (future implementations may consider them jointly) the 90%-credibility constraints have been set to $\Delta M_{\rm f}/\bar{M}_{\rm f} = 0.02^{+0.20}_{-0.17}$ and $\Delta\chi_{\rm f}/\bar{\chi_{\rm f}} = -0.05^{+0.36}_{-0.41}$, which is quite consistent with the expected values $\Delta M_{\rm f}/\bar{M}_{\rm f} = 0$ and $\Delta\chi_{\rm f}/\bar{\chi_{\rm f}} = 0$ from general relativity [10]. Other statistical interpretations of the data give similar consistent results.

6.3 No-hair conjecture

The no-hair theorem states that all black-hole solutions in general relativity can be completely described by three quantities: mass, spin and electric charge. All other information are lost behind the event-horizon and are therefore inaccessible for external observers. In other words, every stationary black hole solution can be described by the Kerr-Newman metric, which is the following

$$\mathrm{d}s^2 = -\Big(\frac{\mathrm{d}r^2}{\Delta} + \mathrm{d}\theta^2\Big)\rho^2 + (c\mathrm{d}t - a\sin^2\theta\,\mathrm{d}\phi)^2\frac{\Delta}{\rho^2} - ((r^2+a^2)\mathrm{d}\phi - ac\mathrm{d}t)^2\frac{\sin^2\theta}{\rho^2},$$

where (r, θ, ϕ) are spherical coordinates. The parameters of the metric are all determined by the mass M of the black hole, its angular momentum J and its electric charge Q:

$$a = \frac{J}{M}, \qquad \rho^2 = r^2 + a^2\cos^2\theta, \qquad \Delta = r^2 - 2Mr + a^2 + Q^2.$$

Thus these three quantities uniquely determine the most general spacetime of a single unperturbed black hole. This theorem hasn't been proofed yet, so it is often called the no-hair conjecture.

When it comes to real astrophysical black holes the electric charge can be neglected and so a black hole is described only by its mass and spin. Once the black hole has become static it is hard to study it experimentally. However, we can use the last phase of a BBH merger, the ringdown, and see if its oscillations are completely described by mass and spin. As the black hole gradually relaxes into the final Kerr state, it damps by oscillating in a set of quasinormal modes (QNMs) while emitting gravitational waves. In previous studies this ringdown test was done using data from late times after the signal peak. This was due to concerns about high non-linearities surrounding the BBH merger at its peak. However, recent studies have shown that already shortly after the peak the signal is dominated by the ringdown overtones [20], [24]. These are the QNMs with the fastest decay rates and highest amplitudes near the peak of the dominant $l = m = 2$ spherical harmonic. In [24] measurements of the first overtone yields agreement with the no-hair conjecture at the $\sim 20\%$ level.

7 Conclusion

We gave a theoretical overview of gravitational waves deriving their solution from linearized gravity. We pointed out that according to general relativity these waves have only two tensor polarization modes and travel at the speed of light. Furthermore, the postulated graviton should be massless. We conclude that the first measurements of gravitational wave events with data from LIGO and Virgo don't show any significant deviations from the theory of general relativity. First analyses of polarization content confirm that models of pure tensor polarization are more likely than models with pure vector or scalar polarizations. However, real alternative theories would most likely have mixed polarization states. These could be tested in future with the help of the stochastic gravitational wave background. First long-time observations couldn't detect any background signal, but could instead place upper bounds on each polarization content of the gravitational-wave background. A very important step in testing the speed of gravitational waves has been reached in 2017 with the first combined measurement of

gravitational (GW170817 by LIGO and Virgo) and electromagnetic (GRB170817 by Fermi) detection from a single source. This detection was able to further constrain the deviations of the speed of gravitational waves from the speed of light. In a phenomenological approach for alternative dispersion relations the Lorentz-violating parameters could be restricted, which helped to put upper bounds on the graviton mass. Also theories of higher-dimensional gravity have been restricted successfully while confirming consistency with the number of spacetime dimensions of general relativity. Tests of the residual waveform after subtracting the best-fit waveform don't show any noteworthy deviations from expectations. Furthermore, the inferred mass and spin from the inspiral and postinspiral phase of a BBH merger are equal, as predicted from theory. In addition to that, the no-hair conjecture still seems to hold to the best of our knowledge.

The future of gravitational waves looks bright. LIGO and Virgo have fulfilled all expectations and granted new powerful insights in the strong-field regime of spacetime. However, the implementation of future detectors will make it possible to test general relativity on an even higher level. KAGRA (Kamioka Gravitational Wave Detector) is already operational and others, like LIGO-India, LISA (Laser Interferometer Space Antenna), LIGO Voyager and more, will follow in the next years. As the detector sensitivities improve, we can expect new results, such as detecting the stochastic gravitational-wave background, which might give insights into the early universe [31], and measuring the low-amplitude overtones, which will provide stronger tests of the postinspiral BBH phase. While LIGO and Virgo are limited in their ability to discern the polarization of gravitational-wave transients, the construction of additional detectors will help to break existing degeneracies and allow for increasingly precise polarization measurements. With the help of LISA, which is expected to come operational in the 2030s, not only will we able to make better observations of the strong-field regime [22], but also measurements of the propagation of gravitational waves will increase in precision and accuracy. New methods on constraining the graviton speed might be implemented [13].

A Gauge symmetry

Under the assumption that the metric $g_{\mu\nu}$ is only a small perturbation of the Minkowski metric we decomposed it into $g_{\mu\nu} = \eta_{\mu\nu} + h_{\mu\nu}$ with $|h_{\mu\nu}| \ll 1$. However, this decomposition is not unique, in the sense that there is a whole family of perturbations $h_{\mu\nu}$ satisfying this condition. These perturbations are connected by a gauge symmetry This is a powerful tool which removes redundant degrees of freedom and lets us choose a simple and elegant form of h. In this section we show a way to see that (4) is indeed a symmetry transformation which leaves the condition invariant, as presented in [17].

Let us consider two pseudo-Riemannian manifolds $(\bar{\mathcal{M}}, \eta)$ and $(\mathcal{M}, g)$. The first one describing the linearized world with the Minkowski metric and the second one describing the real world with a generic metric. Now consider the diffeomorphisms

$$\phi : \bar{\mathcal{M}} \to \mathcal{M}$$

which naively associates the "right" points to each other. There is a naturally associated tangent map ("push-forward")

$$\phi_* : \mathcal{T}\bar{\mathcal{M}} \to \mathcal{T}\mathcal{M}$$

which takes vector fields on the tangent bundle of the linearized manifold and maps them to vector fields on the tangent bundle of the real manifold. Furthermore there is also a cotangent map ("pull-back")

$$\phi^* : \mathcal{T}^*\bar{\mathcal{M}} \to \mathcal{T}^*\mathcal{M}.$$

The metric g is a 2-form, so a tensor field $g \in \mathcal{T}^0_2(\mathcal{M})$. The cotangent map can act on this metric to give a 2-form on $\bar{\mathcal{M}}$

$$\phi^* g \in \mathcal{T}^0_2(\bar{\mathcal{M}})$$

defined through

$$(\phi^* g)(X, Y) = g(\phi_* X, \phi_* Y),$$

where X and Y are two vector fields on $\bar{\mathcal{M}}$. Now we are able to formally define the perturbation as the difference between the pull-back of g and the Minkowski metric

$$h := (\phi^* g) - \eta. \tag{23}$$

Now that we defined what a perturbation is we need to find a family of perturbations parametrized by some parameter ε. Therefore we introduce the flow

$$\psi_\varepsilon : \bar{M} \to \bar{M}$$

which is a 1-parametric group of diffeomorphisms satisfying $\psi_t \circ \psi_s = \psi_{t+s}$ for every $s, t \in \mathbb{R}$. This flow naturally defines a vector field

$$\xi : \mathcal{F}(\mathcal{M}) \to \mathbb{R}$$

$$\xi(f) = \frac{\mathrm{d}}{\mathrm{d}\varepsilon}(f \circ \psi_\varepsilon)\Big|_{\varepsilon=0}.$$

Next consider the parametrized perturbation

$$\begin{aligned} h^{(\varepsilon)} &= [(\phi \circ \psi_\varepsilon)^* g] - \eta \\ &= [\psi_\varepsilon^* (\phi^* g)] - \eta. \end{aligned}$$

Inserting $\phi^* g = h + \eta$ gives

$$\begin{aligned} h^{(\varepsilon)} &= [\psi_\varepsilon^* (h + \eta)] - \eta \\ &= \psi_\varepsilon^*(h) + \psi_\varepsilon^*(\eta) - \eta \\ &= \psi_\varepsilon^*(h) + \varepsilon \left[\frac{\psi_\varepsilon^*(\eta) - \eta}{\varepsilon} \right]. \end{aligned}$$

In the limit $\varepsilon \to 0$ we find

$$h^{(\varepsilon)} = h + \varepsilon \mathcal{L}_\xi \eta. \tag{24}$$

The first term follows simply from the flow condition $\psi_0 = \psi_0 \circ \psi_0 = 1$, while the second term is just the definition of Lie derivative of the tensor field η in direction of the vector field ξ. We found that all small perturbations of the metric are connected by the difference of a Lie derivative along some vector field ξ. This is a beautiful result. Similarly to electromagnetism where the gauge transformation

$$A'_\mu \to A_\mu + \partial_\mu \lambda$$

leaves the physics invariant for every scalar field λ, in linearized gravity the gauge transformation is given by the Lie derivative along ξ.

So far we have used a coordinate-free approach. In order to get to the form in (5) we need to introduce a set of charts x^μ on $\bar{\mathcal{M}}$. Then the diffeomorphisms ψ_ε define the maps

$$\psi_\varepsilon : x^\mu \mapsto y^\mu := (\psi_\varepsilon(x))^\mu.$$

The expansion around $\varepsilon = 0$ gives

$$y^\mu(\varepsilon) = x^\mu + \varepsilon \xi^\mu + \mathcal{O}(\varepsilon^2)$$

and thus

$$\frac{\partial^2 y^\mu}{\partial x^\nu \partial \varepsilon}\bigg|_{\varepsilon=0} = \xi^\mu_{,\nu}. \tag{25}$$

The pullback of a tensor field in coordinates is given by

$$(\psi_\varepsilon^* \eta)_{\mu\nu} = \eta_{\alpha\beta} \frac{\partial y^\alpha}{\partial x^\mu} \frac{\partial y^\beta}{\partial x^\nu}$$

and the computation of the Lie derivative yields

$$\begin{aligned}(\mathcal{L}_\xi \eta)_{\mu\nu} &= \frac{\mathrm{d}}{\mathrm{d}\varepsilon} (\psi_\varepsilon^* \eta)_{\mu\nu} \Big|_{\varepsilon=0} \\ &= \frac{\mathrm{d}}{\mathrm{d}\varepsilon} \eta_{\alpha\beta} \Big|_{\varepsilon=0} \frac{\partial y^\alpha}{\partial x^\mu} \frac{\partial y^\beta}{\partial x^\nu} + \eta_{\alpha\beta} \frac{\partial^2 y^\alpha}{\partial \varepsilon \partial x^\mu} \Big|_{\varepsilon=0} \frac{\partial y^\beta}{\partial x^\nu} + \eta_{\alpha\beta} \frac{\partial y^\alpha}{\partial x^\mu} \frac{\partial^2 y^\beta}{\partial \varepsilon \partial x^\nu} \Big|_{\varepsilon=0}.\end{aligned}$$

The first term vanishes since η is constant and by using (25) the last equation becomes

$$(\mathcal{L}_\xi \eta)_{\mu\nu} = \eta_{\alpha\nu} \xi^\alpha_{\ ,\mu} + \eta_{\beta\mu} \xi^\beta_{\ ,\nu} = \xi_{\nu,\mu} + \xi_{\mu,\nu}.$$

Finally we can insert this result into (24) and find gauge transformation in coordinates

$$h^{(\varepsilon)}_{\mu\nu} = h_{\mu\nu} + \varepsilon \xi_{\nu,\mu} + \varepsilon \xi_{\mu,\nu}, \qquad \varepsilon \ll 1. \tag{26}$$

References

[1] Abbott and et al. Gwtc-1: A gravitational-wave transient catalog of compact binary mergers observed by ligo and virgo during the first and second observing runs. *Physical Review X*, 9(3), Sep 2019.

[2] Benjamin P Abbott, R Abbott, TD Abbott, Fausto Acernese, K Ackley, C Adams, T Adams, Paolo Addesso, Rana X Adhikari, Vaishali B Adya, et al. Tests of general relativity with gw170817. *Physical Review Letters*, 123(1):011102, 2019.

[3] Benjamin P Abbott, Rich Abbott, TD Abbott, Fausto Acernese, Kendall Ackley, Carl Adams, Thomas Adams, Paolo Addesso, RX Adhikari, VB Adya, et al. Gw170817: observation of gravitational waves from a binary neutron star inspiral. *Physical Review Letters*, 119(16):161101, 2017.

[4] Benjamin P Abbott, Richard Abbott, TD Abbott, MR Abernathy, Fausto Acernese, Kendall Ackley, Carl Adams, Thomas Adams, Paolo Addesso, RX Adhikari, et al. Observation of gravitational waves from a binary black hole merger. *Physical Review Letters*, 116(6):061102, 2016.

[5] Benjamin P Abbott, Richard Abbott, TD Abbott, F Acernese, K Ackley, C Adams, T Adams, P Addesso, Rana X Adhikari, VB Adya, et al. Gw170814: a three-detector observation of gravitational waves from a binary black hole coalescence. *Physical Review Letters*, 119(14):141101, 2017.

[6] Benjamin P Abbott, Richard Abbott, Thomas D Abbott, Fausto Acernese, K Ackley, C Adams, T Adams, P Addesso, Rana X Adhikari, VB Adya, et al. Search for tensor, vector, and scalar polarizations in the stochastic gravitational-wave background. *Physical Review Letters*, 120(20):201102, 2018.

[7] Benjamin P Abbott, Robert Abbott, TD Abbott, F Acernese, K Ackley, C Adams, T Adams, P Addesso, RX Adhikari, VB Adya, et al. Gravitational waves and gamma-rays from a binary neutron star merger: Gw170817 and grb 170817a. *The Astrophysical Journal Letters*, 848(2):L13, 2017.

[8] BP Abbott, R Abbott, TD Abbott, S Abraham, Fausto Acernese, K Ackley, C Adams, Rana X Adhikari, VB Adya, C Affeldt, et al. Tests of general relativity with the binary black hole signals from the ligo-virgo catalog gwtc-1. *Physical Review D*, 100(10):104036, 2019.

[9] R Abbott, TD Abbott, S Abraham, F Acernese, K Ackley, A Adams, C Adams, RX Adhikari, VB Adya, C Affeldt, et al. Gwtc-2: Compact binary coalescences observed by ligo and virgo during the first half of the third observing run. *arXiv preprint arXiv:2010.14527*, 2020.

[10] R Abbott, TD Abbott, S Abraham, F Acernese, K Ackley, A Adams, C Adams, RX Adhikari, VB Adya, C Affeldt, et al. Tests of general relativity with binary black holes from the second ligo-virgo gravitational-wave transient catalog. *arXiv preprint arXiv:2010.14529*, 2020.

[11] Bruce Allen and Joseph D Romano. Detecting a stochastic background of gravitational radiation: Signal processing strategies and sensitivities. *Physical Review D*, 59(10):102001, 1999.

[12] L Bernus, O Minazzoli, A Fienga, M Gastineau, J Laskar, P Deram, and A Di Ruscio. Constraint on the yukawa suppression of the newtonian potential from the planetary ephemeris inpop19a. *Physical Review D*, 102(2):021501, 2020.

[13] Dario Bettoni, Jose María Ezquiaga, Kurt Hinterbichler, and Miguel Zumalacárregui. Speed of gravitational waves and the fate of scalar-tensor gravity. *Physical Review D*, 95(8):084029, 2017.

[14] Matthias Blau. *Lecture notes on general relativity.* Albert Einstein Center for Fundamental Physics, 2011.

[15] Alessandra Buonanno. Gravitational waves. *arXiv preprint arXiv:0709.4682*, 2007.

[16] Thomas Callister, A Sylvia Biscoveanu, Nelson Christensen, Maximiliano Isi, Andrew Matas, Olivier Minazzoli, Tania Regimbau, Mairi Sakellariadou, Jay Tasson, and Eric Thrane. Polarization-based tests of gravity with the stochastic gravitational-wave background. *Physical Review X*, 7(4):041058, 2017.

[17] Sean M. Carroll. *Spacetime and Geometry: An Introduction to General Relativity.* Cambridge University Press, 2019.

[18] Katerina Chatziioannou, Nicolás Yunes, and Neil Cornish. Model-independent test of general relativity: An extended post-einsteinian framework with complete polarization content. *Physical Review D*, 86(2):022004, 2012.

[19] Abhirup Ghosh, Nathan K Johnson-McDaniel, Archisman Ghosh, Chandra Kant Mishra, Parameswaran Ajith, Walter Del Pozzo, Christopher PL Berry, Alex B Nielsen, and Lionel London. Testing general relativity using gravitational wave signals from the inspiral, merger and ringdown of binary black holes. *Classical and Quantum Gravity*, 35(1):014002, 2017.

[20] Matthew Giesler, Maximiliano Isi, Mark A Scheel, and Saul A Teukolsky. Black hole ringdown: the importance of overtones. *Physical Review X*, 9(4):041060, 2019.

[21] A Goldstein, P Veres, E Burns, MS Briggs, R Hamburg, D Kocevski, CA Wilson-Hodge, RD Preece, S Poolakkil, OJ Roberts, et al. An ordinary short gamma-ray burst with extraordinary implications: Fermi-gbm detection of grb 170817a. *The Astrophysical Journal Letters*, 848(2):L14, 2017.

[22] Scott A Hughes and Kristen Menou. Golden binary gravitational-wave sources: Robust probes of strong-field gravity. *The Astrophysical Journal*, 623(2):689, 2005.

[23] Richard A. Isaacson. Gravitational radiation in the limit of high frequency. ii. nonlinear terms and the effective stress tensor. *Physical Review*, 166:1272–1280, Feb 1968.

[24] Maximiliano Isi, Matthew Giesler, Will M Farr, Mark A Scheel, and Saul A Teukolsky. Testing the no-hair theorem with gw150914. *Physical Review Letters*, 123(11):111102, 2019.

[25] Maximiliano Isi, Matthew Pitkin, and Alan J. Weinstein. Probing dynamical gravity with the polarization of continuous gravitational waves. *Physical Review D*, 96:042001, Aug 2017.

[26] Philippe Jetzer. General relativity. `https://www.physik.uzh.ch/en/teaching/PHY511/HS2019.html`, 2019.

[27] Jose Beltrán Jiménez, Federico Piazza, and Hermano Velten. Evading the vainshtein mechanism with anomalous gravitational wave speed: constraints on modified gravity from binary pulsars. *Physical Review Letters*, 116(6):061101, 2016.

[28] Fang-Yu Li, Hao Wen, Zhen-Yun Fang, Di Li, and Tong-Jie Zhang. Electromagnetic response to high-frequency gravitational waves having additional polarization states: distinguishing and probing tensor-mode, vector-mode and scalar-mode gravitons. *The European Physical Journal C*, 80(9), Sep 2020.

[29] Saeed Mirshekari, Nicolás Yunes, and Clifford M Will. Constraining lorentz-violating, modified dispersion relations with gravitational waves. *Physical Review D*, 85(2):024041, 2012.

[30] Guy D Moore and Ann E Nelson. Lower bound on the propagation speed of gravity from gravitational cherenkov radiation. *Journal of High Energy Physics*, 2001(09):023, 2001.

[31] Joseph D Romano and Neil J Cornish. Detection methods for stochastic gravitational-wave backgrounds: a unified treatment. *Living Reviews in Relativity*, 20(1):2, 2017.

[32] Bernard F Schutz. Gravitational radiation. *arXiv preprint gr-qc/0003069*, 2000.

[33] Steven Weinberg. Photons and gravitons in perturbation theory: Derivation of maxwell's and einstein's equations. *Physical Review*, 138:B988–B1002, May 1965.

[34] Clifford M Will. The confrontation between general relativity and experiment. *Living Reviews in Relativity*, 17(1):1–117, 2014.

[35] Clifford M Will. *Theory and experiment in gravitational physics*. Cambridge university press, 2018.